ChemPubSoc Europe

DOI: 10.1002/chem.201604567

CHEMISTRY A European Journal Full Paper

Rhodium Catalysis |*Hot Paper*|

A Hemilabile and Cooperative N-Donor-Functionalized 1,2,3-Triazol-5-Ylidene Ligand for Alkyne Hydrothiolation Reactions

Ian Strydom,[a] Gregorio Guisado-Barrios,*[b] Israel Fernández,[c] David C. Liles,[a] Eduardo Peris,[b] and Daniela I. Bezuidenhout*[a, d]

Abstract: A series of novel cationic and neutral Rh complexes with an N-donor-functionalized 1,2,3-triazol-5-ylidene (TRZ) ligand (in which the pendant N donor is NHBoc, NH_2, or NMe_2) is described. The catalytic activity of these complexes was evaluated in the hydrothiolation of alkynes. Among the catalysts, a neutral dicarbonyl complex featuring the tethered-NBoc amido-TRZ ligand proved very selective for alkyne hydrothiolation with an aryl thiol. Remarkably, the reaction could be carried out in the absence of pyridine or base additive. In addition, during the reaction, no evidence for oxidative addition of the thiol S–H bond was observed, strongly suggesting a reaction pathway in which a bifunctional ligand is involved. Experimental and theoretical mechanistic investigations suggest a ligand-assisted deprotonation of thiol, hemilabile dissociation of amine from the metal, and thiolate coordination, which is indicative of a different reaction mechanism to those previously reported for related alkyne hydrothiolation reactions.

Introduction

The hydrothiolation of alkynes involves the atom-economical addition of the sulfur and hydrogen atoms of a thiol group across a carbon–carbon unsaturated bond, generating vinyl sulfides. The structural motifs of vinyl sulfides as building blocks for biologically active compounds[1] and polymers[2] have stimulated the development of efficient and selective synthetic methods for these valuable compounds. To this end, recent strategies have included the metal-catalyzed hydrothiolation of unsaturated carbon–carbon bonds, with the advantage of increased chemo-, stereo-, and regioselectivity over metal-free approaches.[3] Depending on the choice of the metal, the selectivity can be directed towards either the *anti*-Markovnikov β-*E*/*Z*-isomers, or the more challenging Markovnikov-type α-vinyl sulfide products, (Scheme 1).[3] Specifically, in the case of rhodium-based catalysts, both α-[4] and β-isomers[2a,5] have been shown to be accessible by subtle electronic parameterization of the coordination sphere of the metal center, markedly influencing the selectivity outcomes of the reaction. As noted in the mechanistic review of hydrothiolation by Castarlenas, Oro, and co-workers, the so-called "chameleonic" Rh complexes generally allow oxidative addition of the thiol to yield a hydrido thiolato species.[3d] This is unlike other metals such as palladium[5e,6] or nickel,[7] for which only the thiolate ligands remain on the active catalytic species.

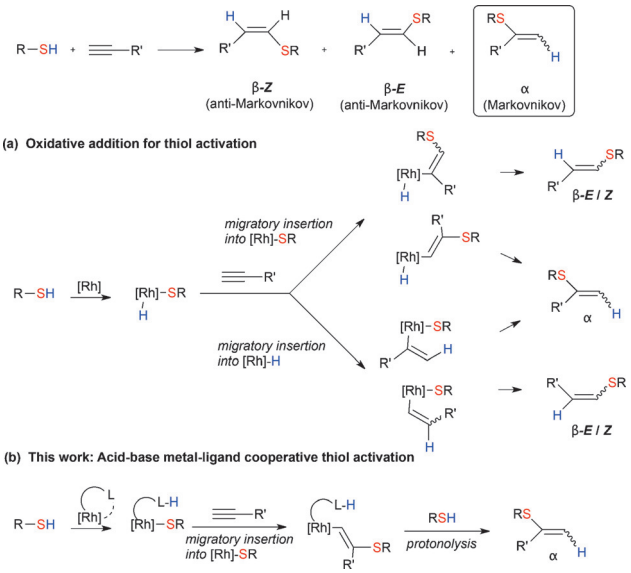

Scheme 1. Thiol activation strategies in rhodium-catalyzed alkyne hydrothiolation.

[a] *I. Strydom, D. C. Liles, Prof. Dr. D. I. Bezuidenhout*
Chemistry Department
University of Pretoria
Private Bag X20, Hatfield 0028, Pretoria (South Africa)

[b] *Dr. G. Guisado-Barrios, Prof. Dr. E. Peris*
Institute of Advanced Materials (INAM), Universitat Jaume I
Avenida Vicente Sos Baynat s/n, 12071 Castellon (Spain)
E-mail: guisado@uji.es

[c] *Prof. Dr. I. Fernández*
Departamento de Química Orgánica I, Facultad de Ciencias Químicas
Universidad Complutense de Madrid
28040 Madrid (Spain)

[d] *Prof. Dr. D. I. Bezuidenhout*
Molecular Sciences Institute, School of Chemistry
University of the Witwatersrand
Johannesburg 2050 (South Africa)
E-mail: daniela.bezuidenhout@wits.ac.za

Supporting information and the ORCID number(s) for the author(s) of this article are available under http://dx.doi.org/10.1002/chem.201604567.

This particular behavior of rhodium catalysts provides the opportunity for the ligand-based direction of the alkyne migratory insertion into either the [Rh]–H or [Rh]–SR bonds for rational control over regioselectivity [Scheme 1(a)]. This approach was elegantly illustrated by the use of 10 equiv excess of pyridine as a directing ligand for Rh-N-heterocyclic carbene (Rh-NHC) complexes, to give the branched Markovnikov products in excellent yields for the hydrothiolation of aryl alkynes with aryl thiols.[4c,d]

To circumvent the use of pyridine additive, we recently reported the synthesis of a donating, monoanionic bis(1,2,3-triazol-5-ylidene)-based C,N,C-type pincer ligand with flanking mesoionic carbene (MIC) moieties.[8] This ligand was a supporting scaffold for [Rh^{I}(CNC)(μ-O$_2$)], an air-stable selective precursor catalyst for the regioselective hydrothiolation of aliphatic alkynes with alkyl thiols.[4a] Similar to the pyrazolylborate rhodium complexes reported by Love et al., however, diminished regioselectivity for the branched α-vinyl sulfides was seen when aryl thiol and aryl alkynes were employed.[4h] It was reasoned that a less encumbered bidentate ligand framework bearing a pendant nitrogen functionality could lead to bifunctional catalyst,[9] behaving as both a directing group and hemilabile ligand. First, negating the use of the pyridine additive, and second, favoring intramolecular activation over oxidative addition through the heterolytic cleavage of the thiol S–H bond [Scheme 1(b)] to improve the regioselectivity of the aryl substrates of alkyne hydrothiolation. Thus, we set out to prepare a series of electron-rich Rh^{I} complexes **A**, **B**, and **C**, containing a tethered N-donor-TRZ ligand (Scheme 2),[10] in which the N-donor is NHBoc, NH$_2$, or NMe$_2$, respectively (TRZ = 1,2,3-triazol-5-ylidene), to exploit the possibility of both hemilability and ligand cooperativity for the activation of the thiol S–H bond.

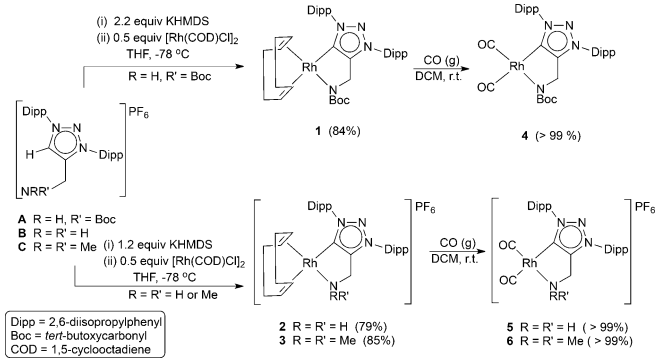

Scheme 2. Synthesis of N-donor functionalized triazolylidene Rh^{I} complexes **1**–**6** (Dipp = 2,6-diisopropylphenyl).

Results and Discussion

Synthesis and characterization of catalyst precursors

The new ligand precursor 1,3-diaryl-1*H*-1,2,3-triazolium salts **A**–**C**[11] were prepared by cycloaddition of the corresponding alkynes and 1,3-bis(2,6-diisopropylphenyl)triaz-1-ene according to an adapted literature procedure.[12] The rhodium complexes **1**–**3** were prepared by reacting the free 1,2,3-triazol-5-ylidene ligands,[13] obtained after deprotonation of the corresponding triazolium salt precursors **A**, **B**, or **C**, respectively, with potassium hexamethyldisilazide (KHMDS), followed by addition to the metal precursor [RhCl(COD)]$_2$ (COD = 1,5-cyclooctadiene) (Scheme 2). The neutral metallocyclic complex **1** [Rh(TRZ-NBoc)(COD)] (84%), was obtained when 2.2 equiv of base were added to precursor **A** prior to metalation. Employing the amino- and dimethylamine-functionalized triazolium salts as precursor ligands (**B** and **C**, respectively) with 1.2 equiv of base led to the isolation of the cationic chelated complexes [Rh(TRZ-NR$_2$)(COD)]$^+$ (**2** and **3**). The dicarbonyl complexes [Rh(TRZ-NBoc)(CO)$_2$] (**4**) and [Rh(TRZ-NR$_2$)(CO)$_2$]PF$_6$ (**5**, R = H; **6**, R = Me) were quantitatively prepared by treatment of the Rh(COD) complexes **1**, **2**, and **3**, respectively, with gaseous CO in dichloromethane (Scheme 2). The [Rh(TRZ-NBoc)(LL)] or [Rh(TRZ-NR$_2$)(LL)]PF$_6$ [LL = COD or (CO)$_2$] metal complexes **1**–**6**, are all air- and moisture-stable. The carbene resonances of the cyclooctadiene complexes **1**–**3** were observed at 162.3 and 164.8 ppm, respectively. The ^{13}C NMR spectra of the dicarbonyl complexes **4**–**6** display the carbene carbon doublet resonances at 164.8 and 169.7 ppm, respectively.

The IR spectra of **4**–**6** show the C–O stretching vibrations (1993, 2068 cm^{-1} for neutral complex **4**; as well as 2027, 2090 cm^{-1} (**5**) and 2031, 2090 cm^{-1} (**6**), for the cationic complexes) within the range of previously reported Rh-TRZ complexes.[14] Crystals suitable for X-ray diffraction could be obtained for complexes **1**–**4** (**2** and **4**, Figure 1; and **1** and **3**, Figure S31 in the Supporting Information), and display pseudo-square planar geometry around the Rh^{I} metal centre (Figure 1). As seen for the carbonyl ligands, the Rh–C$_{carbene}$ bond lengths [2.017(2)–2.045(3) Å] for the structures of **1**–**4** are in accordance with previously reported structures, and are relatively insensitive to changes in the electronic structure around the metal.[14] For the cyclometallated complexes, however, the neutral amido complexes **1** and **4** display the expected shorter Rh–N bond distances [2.130(2) and 2.0924(18) Å, respectively],

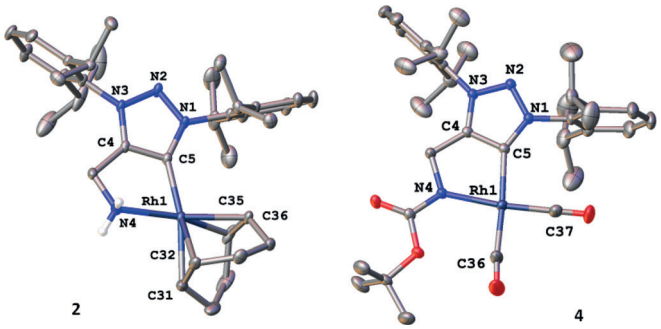

Figure 1. Solid-state structures of complexes **2** and **4** with 50% probability ellipsoids. The PF$_6^-$ counterion and hydrogens (except for the NH$_2$ functional group) were omitted for clarity. Selected bond lengths (Å) and angles (°) for **2**: C5–Rh1 2.029(2); Rh1–N4 2.165(2); Rh1–C31 2.205(2); Rh1–C32 2.173(2); Rh1–C35 2.132(2); Rh1–C36 2.111(2); C5-Rh1-N4 79.22(8); C5-Rh1-C31 164.76(10); C5-Rh1-C32 156.13(10); C5-Rh1-C35 100.60(11); C5-Rh1-C36 98.95(10); for **4**: C5-Rh1 2.036(5); Rh1-N4 2.0924(18); Rh1-C36 1.896(3); Rh1-C37 1.837(3); C5-Rh1-N4 79.69(8); C5-Rh1-C36 175.00(11); C5-Rh1-C37 94.08(10); C37-Rh1-N4 173.68(9).

as compared to the cationic amine complexes **2** and **3** [2.165(2) and 2.222(2) Å, respectively].

Catalytic and mechanistic studies

The catalytic activity of catalysts **1**–**6** was first investigated in the hydrothiolation of 1-hexyne with thiophenol, either in the presence or absence of the weak base K_2CO_3 (2% mol) at 80 °C in deuterated benzene (Table 1). When the reaction was performed in the absence of rhodium catalyst (Table 1, entry 1)

Table 1. Selection of precatalysts in the presence or absence of K_2CO_3 for the model hydrothiolation of 1-hexyne with thiophenol.[a]

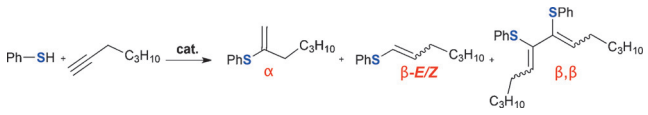

Entry	Catalyst	Conv. [%][c]	Product distribution [%]			
			α	β-*E*	β-*Z*	Coupled bis-β,β
1	K_2CO_3	84	–	52	48	–
2	$[Rh(COD)Cl]_2$[b]	100	4	18	18	60
3	**1**[b]	62	62	34	4	–
4	**1**	94	75	19	6	–
5	**2**[b]	73	94	3	3	–
6	**2**	87	28	6	9	57
7	**3**[b]	58	89	7	4	–
8	**4**[b]	69	97	2	1	–
9	**4**	34	>99	–	–	–
10	**5**[b]	77	97	3	–	–
11	**5**	51[d]	13	24	2	24
12	**6**[b]	54	93	5	2	–

[a] Reactions performed at 80 °C with 2 mol% of catalyst in 0.5 mL C_6D_6, using anisole as an internal standard. [b] 2 mol% of K_2CO_3. [c] Conversion after 24 h calculated by NMR integration based on the internal standard, anisole. [d] Unidentified precipitate observed.

an almost 1:1 mixture of only the linear β-*E* and β-*Z* vinyl sulfide was obtained. This result contrasted with the reaction carried out with $[RhCl(COD)]_2$ in the presence of base (Table 1, entry 2), for which a mixture of the coupled products, the thio-substituted dienes, was obtained (identified as a mixture of the bis-β-*E*,β-*Z*-vinyl sulfide and the bis-β-*Z*,β-*Z*-vinyl sulfide, Figure S36 in the Supporting Information).

In contrast, the metal complexes **1**–**6** displayed excellent selectivity towards the branched vinyl sulfides after 24 h when 2 mol% of K_2CO_3 was added (Table 1, entries 3, 5, 7, 8, 10, and 12); these results are comparable to some of the best rhodium-hydrothiolation catalysts previously reported.[4] In the case of cationic complexes **2** and **5** $[Rh(TRZ\text{-}NH_2)(LL)]^+$ [LL = COD or $(CO)_2$, respectively], the formation of the coupled thio-substituted dienes, in conjunction with the formation of the desired α-vinyl sulfide and the linear products, were seen when the reaction was performed in the absence of K_2CO_3 (Table 1, entries 6 and 11). The presence of this coupled bis-vinyl sulfide product is suggestive of a reaction pathway that includes the presence of two thiolate ligands on the rhodium metal center, similar to the mechanism proposed by Mizobe et al. that follows oxidative addition of two thiolate ligands and concomitant release of molecular hydrogen.[4g]

However, if 2 mol% of the base was added (Table 1, entries 5 and 10), the coupled product was not observed, and a complete selectivity switch was seen to favor the formation of the α-vinyl sulfide product. This is anticipated for a situation in which [Rh]–SR insertion of the alkyne is favored over [Rh]–H insertion.[3d] To rule out the possibility of NH_2-deprotonation of the amino catalyst precursors **2** and **5** by the weak base to yield the neutral amido complexes, the reactions were repeated with the analogous dimethylamine complexes $[Rh(TRZ\text{-}NMe_2)(LL)]^+$ [LL = COD, **3** or $(CO)_2$, **6**]. Similar conversions and selectivity were seen for dimethylamine complexes **3** and **6** (Table 1, entry 7 and 12), as compared to the amino-complex derivatives **2** and **5**, and thus, a possible bifunctional role of the TRZ-NH_2 ligand was dismissed. Instead, base-promoted deprotonation of the thiophenol, and coordination of the resultant thiolate with concomitant de-coordination of the NR_2 (R = H, Me) seemed more likely. To test this hypothesis, stoichiometric reactions were performed in which 1 equiv of thiophenol and K_2CO_3 were added to both complexes **5** and **6** (see the Supporting Information for details). The FT-IR spectra of these complexes displayed a shift of the N–H stretching frequencies for **5** from 3331 and 3285 cm^{-1} to 3311 and 3240 cm^{-1}, respectively, thus indicating dissociation of the NH_2-moiety. For the NMe_2-complex **6**, the $\tilde{\nu}$(CO) bands shifted from 2030 and 2090 cm^{-1} to 2008 and 2076 cm^{-1}, respectively, more closely correlating with the carbonyl vibration bands observed for the neutral Rh^I complex **4** (1993, 2068 cm^{-1}). In both cases, these results point to the hemilabile action of the NR_2 ligands of the cationic complexes, followed by coordination of the deprotonated thiol to yield a neutral Rh^I intermediate. In addition, no Rh–H upfield shift was observed in the ^1H NMR spectra, nor was the $\tilde{\nu}$(Rh–H) vibration observed in the 2200–2300 cm^{-1} region in the IR spectra. This result was also supported by computational calculations of the possible pathways for **5**, comparing: (a) an N-donor function that does not act in a cooperative or hemilabile fashion (Figure S44 in the Supporting Information); (b) a possible N–H effect by deprotonation of the amine group by the weak non-coordinating base combined with a hemilabile functionality (Figure S45); (c) deprotonation of the thiol by the weak base, with no N–H effect and solely a hemilabile function (Figure S46), and oxidative addition of a second thiophenol molecule; and (d) the most energetically favourable pathway, deprotonation of the thiol by the weak base, decoordination of hemilabile NH_2 and substitution by thiophenolate (no oxidative addition and no [Rh]–H intermediate formed; Figure S47).

In contrast, for the neutral amido complexes **1** and **4** [Rh(TRZ-NBoc)(LL)] (LL = COD or $(CO)_2$, respectively), the formation of the mixture of C–C coupled thio-dienes was not observed even in the absence of base (Table 1, entries 4 and 9). Catalyst **4** was proven to be the most selective towards the α-vinyl sulfide, although lower conversions were obtained. A mercury drop-test was performed on catalyst precursor **4** with no significant change in either the conversion or regioselectivi-

ty of the catalyst, thus indicating that a heterogeneous catalytic mode of action can be excluded.[15]

To gain more insight into the reaction mechanism, we decided to explore the stoichiometric reactivity of **4** with substrate thiophenol to investigate the possibility of a cooperative[16] and/or hemilabile catalyst activation mechanism. Both NMR and FT-IR spectra were recorded after addition of the first equivalent of thiophenol, and excess thiophenol in a separate experiment, to **4** [Rh(TRZ-NBoc)$(CO)_2$] in the absence of base, at room temperature (Figures S37–S42 in the Supporting Information). We did not observe any evidence for the formation of Rh-hydride species by NMR and IR spectra, even when recording the spectra after heating at 80° C. In the ^{1}H and ^{13}C NMR spectra, clear evidence for the protonation and dissociation of the resulting NHBoc moiety was seen as well as coordination of the thiolate ligand (Figures S39, S40). The NBoc-CH_2 chemical shift, observed as a singlet peak at 4.71 ppm in Figure 2(a), resonates as a doublet at 4.64 ppm (J = 6.24 Hz), corresponding to the protonated N**H**Boc-CH_2 chemical shift after thiophenol addition [**INT2′**, Figure 2(b)]. Although the N*H*Boc proton could not be unambiguously assigned in the ^{1}H NMR spectrum due to overlap with the aromatic protons, a 2D COSY NMR experiment proved the coupling of the CH_2 group with a chemical shift (N–H) at 6.96 ppm (Figure S41). In the ^{13}C NMR spectrum, a shift of the original Rh–$C_{carbene}$ (δ 170.6, d, J = 45 Hz) and CO resonances (δ 189.7, d, J = 63 Hz; 189.9, d, J = 59 Hz; Figure S38) to δ(Rh–$C_{carbene}$) = 168.2 (d, J = 41 Hz) and δ(CO) = 186.0 (d, J = 65 Hz), 191.0 (d, J = 59 Hz) (Figure S40) is observed. In addition, the coordination of the thiolate is confirmed by the downfield shifted thiophenolate C_{ipso} resonance of the phenyl ring observed at 155.5 ppm, and the downfield shift of the *o*-CH of the phenyl resonating at 7.89 ppm (d, J = 7.24 Hz) and 134.2 ppm, in the ^{1}H and ^{13}C NMR spectra, respectively. The reaction mixture was analyzed by high resolution electrospray-ionization mass spectrometry, and the molecular ion peak of the thiolate complex **INT2′** was observed as $[M-(CO)_2]^+ = [Rh(NHBoc\text{-}TRZ)(SPh)]^+ =$ 729.2746 (calculated exact isotopic mass = 729.2788; Figure S43), consistent with the fragmentation pattern/loss of carbonyl ligands expected for carbonyl complexes during mass spectrometry ionization.

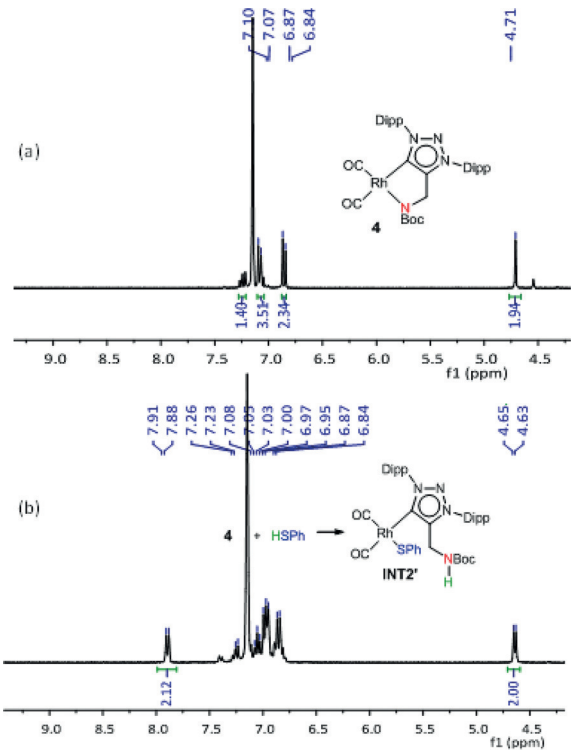

Figure 2. ^{1}H NMR spectra of (a) complex **4** before thiophenol addition and (b) after thiophenol addition (1 equiv) to form Rh-thiolate intermediate **INT2′**.

Similarly, the IR spectrum of **INT2′** after addition of 1 equiv of thiophenol to **4**, supported the protonation and dissociation of the NHBoc moiety, with coordination of the thiolate ligand. The $\tilde{\nu}$(CO) bands observed shifted from 1993 and 2068 cm^{-1} to 1998 and 2060 cm^{-1} after thiophenol addition, and a new broad N–H stretching frequency was observed at 3367 cm^{-1} (absent from the IR spectrum of **4**). The small shift in the carbonyl stretching frequencies indicates that no oxidation of the Rh^{I} metal center had taken place, only exchange of the amido ligand for the thiolato ligand. In addition, the C=O vibration of the Boc-group shifted from 1624 cm^{-1} in **4**, to 1720 cm^{-1} for **INT2′** after thiophenol addition. This stretching frequency more closely resembles the C=O stretching frequency observed for the precursor salt **A** (1715 cm^{-1}), supporting the dissociation of the NHBoc moiety from the Rh^{I} metal center and resultant higher energy NH-stretching frequency. If a second equivalent or excess of thiophenol was added, a mixture of unidentified products was obtained, although no evidence of dithiolate coordination or Rh–H bond formation was obtained in either of the measured NMR or IR spectra, even after heating the reaction mixtures at 80 °C. Importantly, both the IR carbonyl stretching frequencies and the ^{13}C NMR carbene resonance are indicative of a Rh^{I} metal center, and not a Rh^{III} metal center as would be expected as a result of oxidative addition.

Density functional theory (DFT) calculations were additionally carried out to further evaluate the mechanism of the alkyne hydrothiolation reaction catalyzed by rhodium(I) complex **4** (vide supra). To this end, we computed the corresponding reaction profile involving the PhSH and HC≡CMe reactants in the presence of the model Rh^{I} catalyst **4M** (in which the bulky Dipp substituents on the triazolylidene ring were replaced by phenyl groups). The results are shown in Figure 3, which summarizes the corresponding relative free energies (ΔG_{298}, at 298 K) computed at the dispersion corrected B3LYP-D3/def2-SVP level (see computational details below).

From the data in Figure 3, it can be suggested that the process begins with the formation of the initial intermediate **INT1**, characterized by the occurrence of an intermolecular hydrogen bond involving the PhSH reactant and the NBoc moiety of the catalyst. Once this initial intermediate is formed, facile thiolate/NHBoc ligand displacement occurs to produce the Rh^{I} complex **INT2**. The ease of this ligand exchange becomes evident in view of the high exergonicity (ΔG_R = −18.4 kcal mol^{-1} from the separate reactants) and the rather

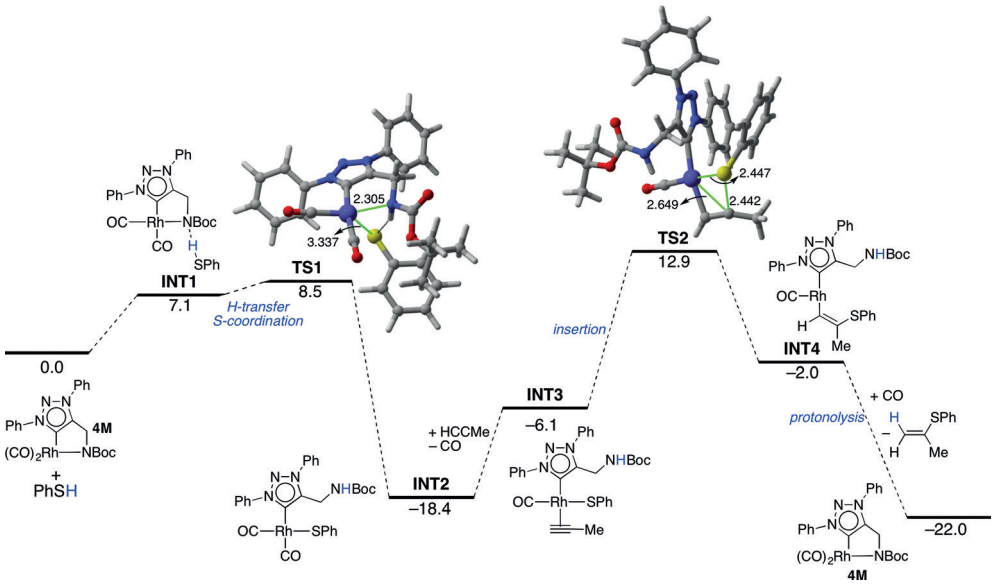

Figure 3. Computed reaction profiles for the reaction of PhSh and HC≡CMe in the presence of model catalyst **4M**. Relative free energies (ΔG_{298}, at 298 K) and bond lengths are given in kcal mol^{-1} and angstroms, respectively. All data have been computed at the B3LYP-D3/def2-SVP level.

low activation barrier ($\Delta G^{\neq} = 1.4$ kcal mol^{-1}, via **TS1**) computed for this reaction step. Endergonic replacement of a CO ligand by the alkyne occurs next to produce intermediate **INT3** ($\Delta G_R = 12.3$ kcal mol^{-1}).[17]

Following this intermediate, insertion of the thiolate ligand into the coordinated alkyne takes place leading to the alkenyl-Rh^{I} complex **INT4**. This slightly endergonic step ($\Delta G_R = 4.1$ kcal mol^{-1}) occurs through the transition state **TS2**, a saddle point associated with the concomitant formation of the new C–S bond and Rh–S cleavage ($\Delta G^{\neq} = 19.8$ kcal mol^{-1}). Final protonolysis of the Rh–C bond (very likely assisted by a new molecule of PhSH) leads to the formation of the observed alkene regenerating the catalyst by coordination of the previously released CO ligand.

The high exergonicity computed for this final step ($\Delta G_R = -20$ kcal mol^{-1}) compensates for the previous endergonic insertion reaction and drives the complete catalytic cycle forward. The proposed reaction mechanism (without considering external base) given in Figure 4, thus includes the dissociation of the hemilabile protonated ligand and thiolate coordination to the metal center to form **INT2′**.

The spectroscopic detection of this intermediate is compatible with its computed thermodynamic stability (see above). Subsequent alkyne coordination by replacing one of the carbonyl ligands (**INT3′**), is followed by alkenyl binding to the metal center (**INT4′**) after the thiolate group migration. Finally, protonolysis, either by a second thiophenol molecule (Path 1, Figure 4) or by deprotonation of the pendant NHBoc ligand (Path 2, Figure 4), yields the vinyl sulfide product and catalyst. In a final stoichiometric reaction, 1 equivalent of alkyne was added to the stoichiometric reaction mixture (**4** + HSPh → **INT2′**), but did not lead to product formation, even after heating to 80 °C. For this reason, it can be concluded that protonolysis of the alkenyl complex **INT4′** by a second thiophenol molecule is more likely (Path 1, Figure 4). Repetition of the stoichiometric reaction with 1 equiv of K_2CO_3 yielded the same results.

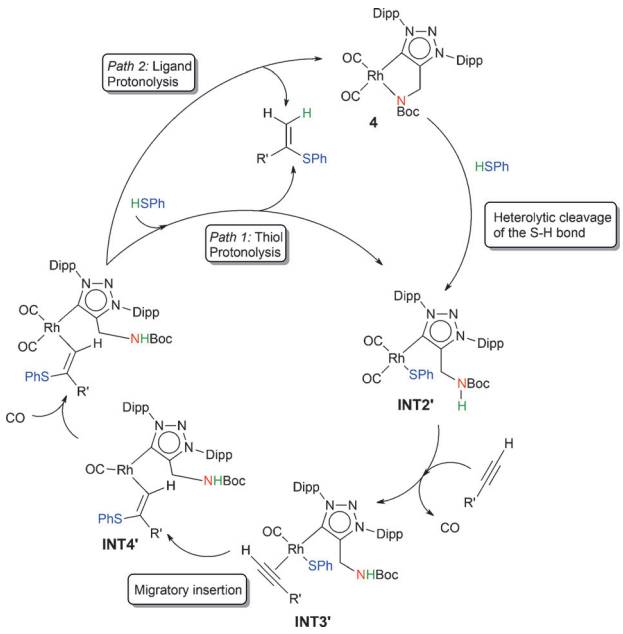

Figure 4. Proposed mechanism incorporating an acid-base metal-ligand cooperative thiol activation, and two possible protonolysis pathways.

In addition, an analysis of Table 1 reveals that in the case of metal complex **2**, the lack of ligand-assisted deprotonation of the thiophenol, can only be circumvented by using a catalytic amount of base to achieve excellent regioselectivity. The evidence for ligand-assisted deprotonation of the thiophenol by **4** prompted us to widen the scope of both aliphatic and aryl substrates with various functional groups for the base-free

Table 2. Scope of the base-free hydrothiolation of terminal alkynes with thiophenol using catalyst precursor **4**.[a]

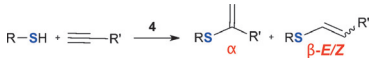

Entry	R	R′	Conv. [%][b]	Product distribution [%]	
				α	β-*E*/*Z*
1	Ph	Ph	43[c]	>99	–
2[d]	Ph	Ph	63	93	7
3	$(CH_2)_4CH_3$	Ph	40	71	29
4	$(CH_2)_4CH_3$	$(CH_2)_4CH_3$	23	98	2
5	Ph	CH_2NH_2	79	86	10[c]
6	Ph	CH_2NMe_2	57	82	18
7	Ph	CH_2NHBoc	91	80	16[d]
8	Ph	CH_2OH	88	86	14
9	Ph	Mes	49	>99	–
10	Ph	Fc	88	97	3

[a] Reactions performed at 80 °C with 2 mol% of **4** in 0.5 mL C_6D_6, using anisole as an internal standard. [b] Conversion calculated after 24 h based on NMR integration of the internal standard, anisole. [c] Unidentified precipitate observed. [d] An additional 4% unidentified byproduct was observed. [e] 2 mol% of K_2CO_3 added. Fc = ferrocene.

hydrothiolation reaction (Table 2), using complex **4** as catalyst. Again, no coupled bis-β,β-vinyl sulfide products were observed, and the reaction was selective for the branched α-vinyl sulfides, thus demonstrating the good functional group tolerance exhibited by the catalyst. Addition of 2 mol% of K_2CO_3 (Table 2, entry 2) leads to an increase in the yield of the reaction, but as previously observed (Table 1, entries 8 and 9), this is accompanied by a slight decrease in selectivity. Notably, the strategy of using a bidentate, hemilabile ligand in a cooperative[16] fashion to deprotonate and activate the substrate thiol (especially thiophenol) proved successful in preventing Rh–H formation, so that alkyne insertion into the resultant Rh–SR bond favors α-isomer product formation.

Conclusion

The performance of a range of cationic and neutral bidentate N-donor functionalized 1,2,3-triazol-5-ylidene Rh^I complexes as catalyst precursors for the alkyne hydrothiolation reaction was investigated. The strategy of combining an electron-donating (TRZ) bidentate ligand with a tethered coordinating N-moiety was followed, as a design approach to yield a catalyst that activates the substrate thiol through deprotonation by the ligand. In addition, direction of the site of attack of the incoming substrate thiol, and insertion of the alkyne substrate into the resulting [Rh]–SR bond for improved Markovnikov-addition regioselectivity of the hydrothiolation reaction, were targeted. For the cationic N-donor (TRZ-NH_2) complexes **2** and **5**, no evidence for a ligand-assisted bifunctional reaction mechanism for the catalytic hydrothiolation could be found, which is supported by the similar results obtained for the dimethylamino analogues **3** and **6**. Instead, stoichiometric and computational studies indicated only the hemilabile action of the NR_2 moiety. In contrast, the neutral amido complexes **1** and **4** demonstrated ligand-assisted activation of the thiol substrates to circumvent the use of the pyridine directing ligand or base in the hydrothiolation reaction. A pathway that includes thiol deprotonation by the pendant amido of the triazolylidene ligand, and hemilabile dissociation of the ligand N-donor was postulated for catalyst precursor **4**, following spectroscopic and computational studies. Excellent regioselectivity towards the branched vinyl sulfide products was shown by catalyst precursor **4**, yielding the notoriously harder-to-come-by α-vinyl sulfides with aryl substituents, specifically for the case in which both alkyne and thiol substrates contain aromatic substituents.

Experimental Section

All air- and moisture-sensitive synthetic procedures were performed under a dinitrogen or argon atmosphere using standard Schlenk techniques. All solvents were purified and distilled over Na (hexane, diethylether, benzene and THF) or CaH_2 (dichloromethane and acetonitrile) under N_2 atmosphere. Bruker AVANCE III-300.12 MHz or 400.21 MHz spectrometers were used for NMR experiments. Chemical shifts (δ) are reported in ppm, downfield from TMS and referenced to the residual solvent chemical shifts. Coupling constants (*J*) are reported in Hz. The NMR spectra were analysed using MNova (Mestrelab research) and the residual solvent chemical shifts were chosen as the default reference shifts in the software. Solution FT-IR spectra [ν<Ü=>(CO)] were recorded on a Bruker ALPHA FT-IR spectrophotometer with a NaCl cell, using CH_2Cl_2 as solvent. The range of absorption measured was from 4000–600 cm^{-1}. Mass spectral analyses were performed on a Waters Synapt G2 HDMS by direct infusion at 5 μL min^{-1} with positive-electron spray as the ionization technique. The *m/z* values were measured in the range of 400–1500 with acetonitrile as solvent for **1**–**4**, and dichloromethane for **5** and **6**. Prior to analysis, a 5 mM sodium formate solution was used to calibrate the instrument in resolution mode.

Preparation of complexes 1–3: A Schlenk tube in the glove box was charged with the precursor triazolium salt **A**[11] (1.40 g, 2.1 mmol) and 2.2 equiv KHMDS (0.93 mg, 4.6 mmol). Freshly distilled, deoxygenated THF (ca. 15 mL) was cannula transferred into this Schlenk tube at −78 °C. The solution was stirred at this temperature for about 30 min, before allowing to warm up to −50 °C. The deprotonated NBoc-functionalized carbene was then slowly transferred dropwise (by cannula) into a THF suspension of 0.5 equiv $[Rh(COD)Cl]_2$ (0.54 g, 1.1 mmol) at −78 °C. The reaction mixture was stirred overnight while slowly allowing to warm up to RT. The solvent was evaporated to complete dryness in vacuo followed by extraction with hexanes, to yield **1**. Crystallization from a dichloromethane solution layered with hexane, yielded crystals of **1** suitable for X-ray diffraction.

Cationic complexes **2** and **3** were prepared using a similar procedure to that described above. Ligand precursors **B** (1.00 g, 1.8 mmol) or **C** (1.10 g, 1. 9 mmol)[11] with 1.2 equiv of KHMDS were used for the synthesis of **2** and **3**, respectively.

[Rh(TRZ-NBoc)(COD)] (1): Yellow powder. Yield: 1.30 g (84%). ^1H NMR[18] (300 MHz, $CDCl_3$): δ 7.47 (dd, 2H, J=7.82 Hz, H_9), 7.26, 7.23 (d, 2H, J=7.80 Hz, $H_{8,10}$), 5.38 (br, 2H, $H_{20,23}$), 4.10 (s, 2H,H_{16}) 3.35 (br, 2H, $H_{20,23}$), 2.52 (sept, 2H, J=6.75 Hz, $H_{12,14}$), 2.25 (m, 2H+2H, $H_{21,22}+H_{12,14}$), 2.10, 1.80, 1.67 (br m, 6H, $H_{21,22}$) 1.37 (s, 9H, H_{19}), 1.35 (d, J=6.79 Hz, 6H, $H_{13,15}$), 1.23, 1.06, 1.03 ppm (d, 18H, J= 6.78, 6.80, 6.90 Hz, $H_{13,15}$); $^{13}C\{^1H\}$ NMR (75 MHz, $CDCl_3$):[18] δ 164.3 (C_{17}), 162.3 (d, J=51.6 Hz, C_5), 157.3 (C_4), 145.2 ($C_{7,11}$), 134.6, 131.1 (C_9), 131.7, 131.6 (C_6), 124.5, 123.6 ($C_{8,10}$), 95.8, 65.5 ($C_{20,23}$) 65.8 (C_{18}),

49.7 (C_{16}), 28.5 (C_{19}), 28.7, 28.6 ($C_{12,14}$), 31.7, 29.4, 28.9, 26.4, 23.8, 22.4 ppm ($C_{13,15,\ 21,\ 22}$); HRMS: *m/z*: $[M+H]^+$ calcd: 729.3615; found: 729.3607.

[Rh(TRZ-NH$_2$)(COD)]PF$_6$ (2): Yellow powder. Yield: 1.10 g, 79%. ^{1}H NMR[18] (300 MHz, CD_2Cl_2): δ 7.63, 7.56 (dd, 1H, J=7.85 Hz, 7.82 Hz, H_9), 7.41, 7.35 (d, 2H, J=7.86 Hz, 7.83 Hz, $H_{8,10}$), 4.63 (m, 2H, $H_{21,22}$) 3.89 (t, 2H, J=6.13 Hz, H_{16}), 3.68 (m, 2H, $H_{21,22}$), 3.61 (bt, 2H, H_N) 2.45 (sept, 2H, J=6.79 Hz, $H_{12,\ 14}$)), 2.22 (m, 4H+2H, $H_{21,22}+H_{12,14}$), 1.89, 1.79 (m, 2H, $H_{21,22}$), 1.43, 1.30, 1.15, 1.11 ppm (d, 24H, J=6.77 Hz, 6.83 Hz, 6.81 Hz, 6.89 Hz, $H_{13,15}$); ^{13}C{^{1}H} NMR[18] (75 MHz, CD_2Cl_2): δ 164.8 (d, J=51.9 Hz, C_5) 156.8 (C_4) 145.6, 145.5 ($C_{7,11}$), 134.7, 130.4 (C_9), 133.2, 132.3 (C_6), 125.6, 124.7 ($C_{8,10}$), 93.7 (d, J=8.26 Hz, C_{20}) 74.2 (d, J=13.1 Hz, C_{23}) 41.8 (C_{16}), 32.2, 29.5 ($C_{12,14}$), 25.7, 25.1, 23.9, 23.2 ppm ($C_{13,15,21,22}$); ^{31}P NMR (121 MHz, CD_2Cl_2): δ = −144.5 ppm (hept, J=711.1 Hz); ^{19}F NMR (282 MHz, CD_2Cl_2): δ −72.9 ppm (d, J=711.2 Hz); HRMS: *m/z*: $[M-PF_6]^+$ calcd: 629.3090; found: 629.3089.

[Rh(TRZ-NMe$_2$)(COD)]PF$_6$ (3): Yellow powder. Yield: 1.30 g, 85%. ^{1}H NMR[18] (300 MHz, CD_2Cl_2): δ 7.67, 7.60 (dd, 1H, J=7.84 Hz, 7.82 Hz, H_9), 7.41, 7.35 (d, 2H, J=7.85 Hz, 7.83 Hz, $H_{8,10}$), 4.55 (m, 2H, H_{18}) 3.65 (s, 2H, H_{16}), 3.62 (m, 2H, H_{21}), 2.68 (s, 6H, H_{17}) 2.28 (m, (2H + 2H) + (2H+2H), $H_{12,\ 14}$ + $H_{19,20}$), 1.91, 1.77 (m, 2H+ 2H, $H_{19,20}$), 1.48, 1.31, 1.17, 1.14 ppm (d, 24H, J=6.81 Hz, 6.86 Hz, 6.80 Hz, 6.88 Hz, $H_{13,15}$); ^{13}C{^{1}H} NMR[18] (75 MHz, CD_2Cl_2): δ 164.8 (d, J=52.1 Hz, C_5) 152.2 (C_4) 145.6, 145.3 ($C_{7,11}$), 134.3, 129.9 (C_6), 133.4, 132.6 (C_9), 125.7, 124.9 ($C_{8,10}$), 96.2 (d, J=8.37 Hz, C_{18}) 73.3 (d, J=13.5 Hz, C_{21}) 60.8 (C_{16}), 50.2 (C_{17}) 31.9, 29.1 ($C_{19,20}$), 29.8, 29.6 ($C_{12,14}$), 26.1, 25.5, 23.8, 22.8 ppm ($C_{13,15}$); ^{31}P NMR (121 MHz, CD_2Cl_2): δ −144.5 ppm (sept, J=710.7 Hz); ^{19}F NMR (282 MHz, CD_2Cl_2): δ −73.2 ppm (d, J=710.8 Hz); HRMS: *m/z*:$[M-PF_6]^+$ calculated: 629.3090; observed: 629.3089.

Preparation of complexes 4–6: The dicarbonyl complexes **4**, **5**, and **6** were prepared from the corresponding COD complexes **1** (0.54 g, 0.74 mmol), **2** (0.47 g, 0.61 mmol), or **3** (0.32 g, 0.40 mmol), respectively, by dissolving the precursor metal complex in about 20 mL dichloromethane. CO gas was bubbled through the solution at room temperature for about 5 min until the color of the solution ceased to lighten. The solution was stirred for about 15 min in the CO atmosphere, before the solvent was evaporated. Subsequent washing with hexanes yielded the pure complexes.

[Rh(TRZ-NBoc)(CO)$_2$] (4): Pale yellow powder. Yield: 0.50 g, 99%. ^{1}H NMR[18] (300 MHz, CD_2Cl_2) δ 7.58 (dd, 2H, J=7.98 Hz, H_9), 7.39, 7.38 (d, 4H, J=7.80 Hz, 6.97 Hz, $H_{8,10}$), 4.17 (s, 2H,H_{16}), 2.46, 2.31 (sept, 4H, $H_{12,14}$), 1.45 (s,9H,H_{19}), 1.36, 1.28, 1.16, 1.13 ppm (d, 24H, J=6.82 Hz, 6.75 Hz, 6.91 Hz, 6.73 Hz, $H_{13,15}$); ^{13}C{^{1}H} NMR[18] (75 MHz, CD_2Cl_2) δ 189.4, 188.9 (d, J=61.5 Hz, 59.2 Hz, $C_{20,21}$), 169.7 (d, J=44.4 Hz, C_5), 163.0 (C_4), 158.3 (C_{17}) 146.0, 145.8 ($C_{7,11}$), 135.1, 131.1 (C_9), 132.7, 132.1 (C_6), 125.9, 125.5 ($C_{8,10}$), 81.2 (C_{18}), 35.8 (C_{16}), 29.9, 29.7, 28.4 (C_{19}), 25.9, 24.9. 24.0, 22.9 ppm, ($C_{13,15}$); FTIR (CH_2Cl_2): $\tilde{\nu}$(CO) = 1624, 1993, 2068 cm^{-1}, $\tilde{\nu}$ (NH) = 3367 cm^{-1}; HRMS: *m/z*: $[M-CO+MeCN]^+$ calcd: 725.7365; found: 725.7384.

[Rh(TRZ-NH$_2$)(CO)$_2$]PF$_6$ (5): Pale yellow powder. Yield: 0.44 g, 100%. ^{1}H NMR[18] (300 MHz, CD_2Cl_2): δ 7.66, 7.61 (dd, 1H, J=7.87, 7.83, H_9), 7.43, 7.40 (d, 2H, J=7.59, 7.66, $H_{8,10}$), 4.30 (b, 2H, H_N) 4.09 (t, 2H, J=5.88, H_{16}), 2.36, 2.24 (sept, 2H, J=6.86, 6.84, $H_{12,\ 14}$), 1.36, 1.31, 1.17, 1.15 ppm (d, 24H, J=6.81, 6.82, 7.44, 7.15, $H_{13,15}$); ^{13}C{^{1}H} NMR[18] (75 MHz, CD_2Cl_2) δ 185.6, 185.1 (d, J=56.3, 72.5, $CO_{17,18}$) 164.8 (d, J=45.2, C_5) 156.6 (C_4) 145.9, 145.6 ($C_{7,11}$), 134.5, 130.3 (C_6), 133.5, 132.8 (C_9), 125.6, 124.7 ($C_{8,10}$), 42.0 (C_{16}), 29.8, 29.6 ($C_{12,14}$), 25.7, 25.1, 24.0, 23.4 ppm ($C_{13,15}$); ^{31}P NMR (121 MHz, CD_2Cl_2): δ −144.4 ppm (sept, J=712.4 Hz); ^{19}F NMR (282 MHz, CD_2Cl_2) δ −72.5 ppm (d, 712.3 Hz); FTIR (CH_2Cl_2): $\tilde{\nu}$(CO) = 2027, 2090 cm^{-1}; $\tilde{\nu}$(NH) = 3311, 3250 cm^{-1}; HRMS: *m/z*: $[M]^+$ calcd: 577.2050; found: 577.2044.

[Rh(TRZ-NMe$_2$)(CO)$_2$]PF$_6$ (6): Pale yellow powder. Yield: 0.30 g, 100%. ^{1}H NMR[18] (300 MHz, CD_2Cl_2) δ 7.62, 7.57 (dd, 1H, J=7.80, 7.84, H_9), 7.38, 7.34 (d, 2H, J=7.86, 7.87, $H_{8,10}$), 3.76 (s, 2H, H_{16}), 2.95 (s, 6H, H_{17}) 2.23, 2.11 (sept, 2H, J=6.90, 7.00, $H_{12,\ 14}$), 1.30, 1.24, 1.12, 1.10 ppm (d, 24H, J=6.84, 6.85, 8.12, 7.13, $H_{13,15}$); ^{13}C{^{1}H} NMR[18] (CD_2Cl_2, 54.0 ppm) δ 185.7, 184.4 (d, J=58.4, 72.3, $CO_{18,19}$) 168.9 (d, J=45.3, C_5) 154.2 (C_4) 145.5, 145.3 ($C_{7,11}$), 134.0, 129.7 (C_6), 133.8, 133.0 (C_9), 125.7, 125.2 ($C_{8,10}$), 60.9 (C_{16}), 53.8 (C_{17}), 29.9, 29.7 ($C_{12,14}$), 25.4, 25.0, 23.9, 23.4 ppm ($C_{13,15}$); ^{31}P NMR (121 MHz, CD_2Cl_2) δ −144.5 ppm (sept, J=711.0); ^{19}F NMR (282 MHz, CD_2Cl_2) δ −72.8 ppm (d, 711.1 Hz); FTIR (CH_2Cl_2): $\tilde{\nu}$(CO) = 2031, 2090 cm^{-1}; HRMS: *m/z*: $[M]^+$ calcd: 605.2363; found: 605.2363.

Crystal structure determination: Single crystal X-ray diffraction data were collected on a Bruker Apex II-CCD detector using Mo-K_α radiation (λ = 0.71073 Å). Crystals were selected under oil, mounted on nylon loops then immediately placed in a cold stream of N_2 at 150 K. Structures were solved and refined using Olex2 and SHELXTL. A satisfactory refinement of the crystal structure of complex **4** was only obtained after squeeze methodology was applied to eliminate residual electronic density of the solvent, which could not be refined otherwise.[19] CCDC 1504559 (**A**), 1504560 (**B**), 1504561 (**C**), 1504562 (**2**), and 1504563 (**4**) contain the supplementary crystallographic data for this paper. These data are provided free of charge by The Cambridge Crystallographic Data Centre.

Crystal data for compound 2: $C_{35}H_{50}N_4F_6PRh$ (M = 774.67 g mol^{-1}): monoclinic, space group $P2_1/n$ (no. 14), a = 11.6643(5) Å, b = 12.5642(6) Å, c = 24.8822(11) Å, β = 102.418(2)°, V = 3561.2(3) Å^3, Z = 4, T = 150.15 K, μ(MoKα) = 0.586 mm^{-1}, *Dcalc* = 1.445 g cm^{-3}, 121 530 reflections measured (4.664° ≤ 2Θ ≤ 52.924°), 7330 unique (R_{int} = 0.0460, R_{sigma} = 0.0151) which were used in all calculations. The final R_1 was 0.0330 (I > 2σ(I)) and wR_2 was 0.0893 (all data).

Crystal data for compound 4: $C_{34}H_{45}N_4O_4Rh$ (M = 676.65 g mol^{-1}): triclinic, space group P-1 (no. 2), a = 12.3738(6) Å, b = 12.4127(4) Å, c = 12.5387(6) Å, α = 73.281(4)°, β = 85.620(4)°, γ = 75.727(4)°, V = 1787.46(14) Å^3, Z = 2, T = 293(2) K, μ(MoKα) = 0.517 mm^{-1}, *Dcalc* = 1.257 g cm^{-3}, 55 567 reflections measured (5.882° ≤ 2Θ ≤ 51.994°), 7031 unique (R_{int} = 0.0708, R_{sigma} = 0.0338) which were used in all calculations. The final R_1 was 0.0328 (I > 2σ(I)) and wR_2 was 0.0891 (all data).

DFT calculations: All the calculations reported in this paper were obtained with the GAUSSIAN 09 suite of programs.[20] Electron correlation was partially taken into account using the hybrid functional usually denoted as B3LYP[21] in conjunction with the D3 dispersion correction suggested by Grimme et al.[22] using the double-quality plus polarization def2-SVP basis set[23] for all atoms. This level is denoted B3LYP-D3/def2-SVP. Reactants and products were characterized by frequency calculations,[24] and have positive definite Hessian matrices. Transition structures (TS's) show only one negative eigenvalue in their diagonalized force constant matrices, and their associated eigenvectors were confirmed to correspond to the motion along the reaction coordinate under consideration using the intrinsic reaction coordinate (IRC) method.[25]

Acknowledgements

The authors gratefully acknowledge Ms. Madelien Wooding, University of Pretoria, for the mass spectrometric measurements. G.G.-B. thanks the MINECO for a postdoctoral grant (FPDI-2013–16525) and Generalitat Valenciana (GV/2015/

097) for financial support. E.P and I.F. gratefully acknowledge financial support from the Spanish MINECO-FEDER (CTQ2014-51999-P to E.P. and CTQ2013-44303-P and CTQ2014-51912-REDC to I.F.), UJI (P11B2014-02 to E.P.). D.I.B and I.S. gratefully acknowledge the National Research Foundation, South Africa (NRF 87890, 103698 and 92521), and Sasol Technology R&D Pty. Ltd., South Africa for financial support.

Keywords: 1,2,3-triazol-5-ylidene (trz) · hemilabile · hydrothiolation · mesoionic carbene · rhodium

[1] For selected examples of vinyl sulfides with biological applications, see: a) C. A. Dvorak, W. D. Schmitz, D. J. Poon, D. C. Pryde, J. P. Lawson, R. A. Amos, A. I. Meyers, *Angew. Chem. Int. Ed.* **2000**, *39*, 1664 – 1666; *Angew. Chem.* **2000**, *112*, 1730 – 1732; b) M. Ceruti, G. Balliano, F. Rocco, P. Milla, S. Arpicco, L. Cattel, F. Viola, *Lipids* **2001**, *36*, 629 – 636; c) P. Johannesson, G. Lindeberg, A. Johansson, G. V. Nikiforovich, A. Gogoll, B. Synnergren, M. LeGrèves, F. Nyberg, A. Karlén, A. Hallberg, *J. Med. Chem.* **2002**, *45*, 1767 – 1777; d) Á. Szilágyi, F. Fenyvesi, O. Majercsik, I. F. Pelyvás, I. Bácskay, P. Fehér, J. Váradi, M. Vecsernyés, P. Herczegh, *J. Med. Chem.* **2006**, *49*, 5626 – 5630; e) M. C. Aversa, A. Baratucci, P. Bonaccorsi, F. Marino-Merlo, A. Mastino, M. T. Sciortino, *Bioorg. Med. Chem.* **2009**, *17*, 1456 – 1463.

[2] For selected examples of vinyl sulfides as polymers, see: a) J. Liu, J. W. Y. Lam, C. K. Jim, J. C. Y. Ng, J. Shi, H. Su, K. F. Yeung, Y. Hong, M. Faisel, Y. Yu, K. S. Wong, B. Z. Tang, *Macromolecules* **2011**, *44*, 68 – 79; b) A. B. Lowe, J. W. Chan, in *Functional Polymers by Post-Polymerization Modification*; P. Theato, H.-A. Eds. Klok, Wiley-VCH Verlag GmbH & Co. KGaA: Weinheim, **2013**, pp. 87 – 118; c) B. Yao, J. Mei, J. Li, J. Wang, H. Wu, J. Z. Sun, A. Qin, B. Z. Tang, *Macromolecules* **2014**, *47*, 1325 – 1333; d) I.-T. Trotuş, T. Zimmermann, F. Schüth, *Chem. Rev.* **2014**, *114*, 1761 – 1782.

[3] For recent reviews, see: a) M. Wathier, J. A. Love, *Eur. J. Inorg. Chem.* **2016**, 2391 – 2402; b) A. Dondoni, A. Marra, *Eur. J. Org. Chem.* **2014**, 3955 – 39659; c) R. Chinchilla, C. Nájera, *Chem. Rev.* **2014**, *114*, 1783 – 1826; d) R. Castarlenas, A. Di Giuseppe, J. J. Pérez-Torrente, L. A. Oro, *Angew. Chem. Int. Ed.* **2013**, *52*, 211 – 222; *Angew. Chem.* **2013**, *125*, 223 – 234; e) I. P. Beletskaya, V. P. Ananikov, *Chem. Rev.* **2011**, *111*, 1596 – 1636.

[4] a) G. Kleinhans, G. Guisado-Barrios, D. C. Liles, G. Bertrand, D. I. Bezuidenhout, *Chem. Commun.* **2016**, *52*, 3504 – 3507; b) S. Kankala, S. Nerella, R. Vadde, C. S. Vassam, *RSC Adv.* **2013**, *3*, 23582 – 23588; c) L. Palacios, M. J. Artigas, V. Polo, F. J. Lahoz, R. Castarlenas, J. J. Pérez-Torrente, L. A. Oro, *ACS Catal.* **2013**, *3*, 2910 – 2919; d) A. Di Giuseppe, R. Castarlenas, J. J. Pérez-Torrente, M. Crucianelli, R. Sancho, F. J. Lahoz, L. A. Oro, *J. Am. Chem. Soc.* **2012**, *134*, 8171 – 8183; e) J. Yang, A. Sabarre, L. R. Fraser, B. O. Patrick, J. A. Love, *J. Org. Chem.* **2009**, *74*, 182 – 187; f) L. R. Fraser, J. Bird, Q. Wu, C. Cao, B. O. Patrick, J. A. Love, *Organometallics* **2007**, *26*, 5602 – 5611; g) Y. Misumi, H. Seino, Y. Mizobe, *J. Organomet. Chem.* **2006**, *691*, 3157 – 3164; h) C. Cao, L. R. Fraser, J. A. Love, *J. Am. Chem. Soc.* **2005**, *127*, 17614 – 17615.

[5] a) H. Zhao, J. Peng, M. Cai, *Catal. Lett.* **2012**, *142*, 138 – 142; b) L. D. Field, B. A. Messerle, K. Q. Vuong, P. Turner, *Dalton Trans.* **2009**, 3599 – 3614; c) S. Shoai, P. Bichler, B. Kang, H, Buckley, J. A. Love, *Organometallics* **2007**, *26*, 5778 – 5781; d) S. Burling, L. D. Field, B. A. Messerle, K. Q. Vuong, P. Turner, *Dalton Trans.* **2003**, 4181 – 4191; e) A. Ogawa, T. Ikeda, K. Kimura, J. Hirao, *J. Am. Chem. Soc.* **1999**, *121*, 5108 – 5114.

[6] a) R. Gerber, C. M. Frech, *Chem. Eur. J.* **2012**, *18*, 8901 – 8905; b) V. P. Ananikov, N. V. Orlov, S. S. Zalesskiy, I. P. Beletskaya, V. N. Khrustalev, K. Morokuma, D. G. Musaev, *J. Am. Chem. Soc.* **2012**, *134*, 6637 – 6649; c) T. Mitamura, M. Daitou, A. Nomoto, A. Ogawa, *Bull. Chem. Soc. Jpn.* **2011**, *84*, 413 – 415; d) S. Kodama, A. Nomoto, M. Kajitani, E. Nishinaka, M. Sonoda, A. Ogawa, *J. Sulfur Chem.* **2009**, *30*, 309 – 318; e) V. P. Ananikov, N. V. Orlov, I. P. Beletskaya, V. Khrustalev, M. Y. Antipin, T. V. Timofeeva, *J. Am. Chem. Soc.* **2007**, *129*, 7252 – 7253; f) A. Kondoh, H. Yorimitsu, K. Oshima, *Org. Lett.* **2007**, *9*, 1383 – 1385; g) B. Gabriele, G. Salerno, A. Fazio, *Org. Lett.* **2000**, *2*, 351 – 352; h) J.-E. Bäckvall, A. Ericsson, *J. Org. Chem.* **1994**, *59*, 5850 – 5851; i) H. Kuniyasu, A. Ogawa, K.-I. Sato, I. Ryu, N. Kambe, N. Sonoda, *J. Am. Chem. Soc.* **1992**, *114*, 5902 – 5903.

[7] a) V. P. Ananikov, N. V. Gayduck, N. V. Orlov, I. P. Beletskaya, V. N. Khrustalev, M. Y. Antipin, *Chem. Eur. J.* **2010**, *16*, 2063 – 2071; b) D. A. Malyshev, N. M. Scott, N. Marion, E. D. Stevens, V. P. Ananikov, I. P. Beletskaya, S. P. Nolan, *Organometallics* **2006**, *25*, 4462 – 4470; c) V. P. Ananikov, L. P. Orlov, I. P. Beletskaya, *Organometallics* **2006**, *25*, 1970 – 1977; d) V. P. Ananikov, D. A. Malyshev, I. P. Beletskaya, G. G. Aleksandrov, I. L. Eremenko, *Adv. Synth. Catal.* **2005**, *347*, 1993 – 2001; e) L.-B. Han, C. Zhang, H. Yazawa, S. Shimada, *J. Am. Chem. Soc.* **2004**, *126*, 5080 – 5081.

[8] D. I. Bezuidenhout, G. Kleinhans, G. Guisado-Barrios, D. C. Liles, G. Ung, G. Bertrand, *Chem. Commun.* **2014**, *50*, 2431 – 2433.

[9] For recent reviews, see: a) R. H. Morris, *Acc. Chem. Res.* **2015**, *48*, 1494 – 1502; b) J. R. Khusnutdinova, D. Milstein, *Angew. Chem. Int. Ed.* **2015**, *54*, 12236 – 12273; *Angew. Chem.* **2015**, *127*, 12406 – 12445; c) T. Zell, D. Milstein, *Acc. Chem. Res.* **2015**, *48*, 1979 – 1994; d) S. Kuwata, T. Ikariya, *Chem. Commun.* **2014**, *50*, 14290 – 14300; e) D. Gelman, M. Sanaa, *ACS Catal.* **2012**, *2*, 2456 – 2466; f) B. Askevold, H. W. Roesky, S. Schneider, *ChemCatChem* **2012**, *4*, 307 – 320; g) W. Kaim, *Eur. J. Inorg. Chem.* **2012**, 343 – 348; h) W. I. Dzik, B. de Bruin, *Organomet. Chem.* **2011**, *37*, 46 – 78; i) C. Gunanathan, D. Milstein, *Acc. Chem. Res.* **2011**, *44*, 588 – 602; j) H. Grützmacher, *Angew. Chem. Int. Ed.* **2008**, *47*, 1814 – 1818; *Angew. Chem.* **2008**, *120*, 1838 – 1842.

[10] a) R. Lalrempuia, N. D. McDaniel, H. Müller-Bunz, S. Bernhard, M. Albrecht, *Angew. Chem. Int. Ed.* **2010**, *122*, 9959 – 9962; *Angew. Chem.* **2010**, *49*, 9765 – 9768; b) R. Cao, W. Lai, P. Du, *Energy Environ. Sci.* **2012**, *5*, 8134 – 8157; c) D. Canseco-Gonzalez, A. Petronilho, H. Mueller-Bunz, K. Ohmatsu, T. Ooi, M. Albrecht, *J. Am. Chem. Soc.* **2013**, *135*, 13193 – 13203.

[11] The synthesis, spectroscopic characterization, and single-crystal X-ray structures of the new triazolium salts **A**–**C** are reported in the Supporting Information.

[12] J. Bouffard, B. K. Keitz, R. Tonner, G. Guisado-Barrios, G. Frenking, R. H. Grubbs, G. Bertrand, *Organometallics* **2011**, *30*, 2617 – 2627.

[13] G. Guisado-Barrios, J. Bouffard, B. Donnadieu, G. Bertrand, *Angew. Chem. Int. Ed.* **2010**, *122*, 4869 – 4872; *Angew. Chem.* **2010**, *49*, 4759 – 4762.

[14] a) D. Mendoza-Espinosa, R. González-Olvera, G. E. Negrón-Silva, D. Angeles-Beltrán, O. R. Suárez-Castillo, A. Álvarez-Hernández, R. Santillan, *Organometallics* **2015**, *34*, 4529 – 4542; b) T. V. Q. Nguyen, W.-J. Yoo, S. Kobayashi, *Angew. Chem. Int. Ed.* **2015**, *54*, 9209 – 9212; *Angew. Chem.* **2015**, *127*, 9341 – 9344; c) X. Yan, J. Bouffard, G. Guisado-Barrios, B. Donnadieu, G. Bertrand, *Chem. Eur. J.* **2012**, *18*, 14627 – 14631; d) M. T. Zamora, M. J. Ferguson, M. Cowie, *Organometallics* **2012**, *31*, 5384 – 5395; e) A. Poulain, D. Canseco-Gonzalez, R. Hynes-Roche, H. Müller-Bunz, O. Schuster, H. Stoeckli-Evans, A. Neels, M. Albrecht, *Organometallics* **2011**, *30*, 1021 – 1029; f) P. Mathew, A. Neels, M. Albrecht, *J. Am. Chem. Soc.* **2008**, *130*, 13534 – 13535.

[15] a) D. R. Anton, R. H. Crabtree, *Organometallics* **1983**, *2*, 855 – 859; b) J. A. Widegren, R. G. Finke, *J. Mol. Catal. A* **2003**, *198*, 317 – 341.

[16] a) W. W. N. O, A. J. Lough, R. H. Morris, *Organometallics* **2011**, *30*, 1236 – 1252; b) W. W. N. O, A. J. Lough, R. H. Morris, *Organometallics* **2012**, *31*, 2152 – 2165.

[17] An alternative reaction mechanism involving a related **INT3** having a square pyramidal Rh^{I} cannot be discarded. For related species, see: a) L. D. Field, B. A. Messerle, K. Q. Vuong, P. Turner, *Organometallics* **2005**, *24*, 42414250; b) W. Gil, A. M. Trzeciak, J. J. Ziolkowski, *Organometallics* **2008**, *27*, 4131 – 4138.

[18] See the Supporting Information for full NMR spectra and atom-numbering scheme.

[19] a) O. V. Dolomanov, L. J. Bourhis, R. J. Gildea, J. A. K. Howard, H. Puschmann, *J. Appl. Crystallogr.* **2009**, *42*, 339 – 341; b) M. C. Burla, R. Caliandro, M. Camalli, B. Carrozzini, G. L. Cascarano, L. De Caro, C. Giacovazzo, G. Polidori, D. Siliqi, R. Spagna, *J. Appl. Crystallogr.* **2007**, *40*, 609 – 613; c) G. M. Sheldrick, *Acta Crystallogr. Sect. A* **2008**, *64*, 112 – 122.

[20] Gaussian 09, Revision D.01. M. Frisch, G. Trucks, H. Schlegel, G. Scuseria, M. Robb, J. Cheeseman, G. Scalmani, V. Barone, B. Mennucci, G. Petersson, H. Nakatsuji, M. Caricato, X. Li, H. P. Hratchian, A. F. Izmaylov, J. Bloino, G. Zheng, J. L. Sonnenberg, M. Hada, M. Ehara, K. Toyota, R. Fukuda, J. Hasegawa, M. Ishida, T. Nakajima, Y. Honda, O. Kitao, H. Nakai, T. Vreven, J. J. A. Montgomery, J. E. Peralta, F. Ogliaro, M. Bearpark, J. J. Heyd, E. Brothers, K. N. Kudin, V. N. Staroverov, R. Kobayashi, J. Normand, K. Raghavachari, A. Rendell, J. C. Burant, S. S. Iyengar, J. Tomasi, M. Cossi, N. Rega, N. J. Millam, M. Klene, J. E. Knox, J. B. Cross, V.

Bakken, C. Adamo, J. Jaramillo, R. Gomperts, R. E. Stratmann, O. Yazyev, A. J. Austin, R. Cammi, C. Pomelli, J. W. Ochterski, R. L. Martin, K. Morokuma, V. G. Zakrzewski, G. A. Voth, P. Salvador, J. J. Dannenberg, S. Dapprich, A. D. Daniels, Ö. Farkas, J. B. Foresman, J. V. Ortiz, J. Cioslowski, D. J. Fox, Gaussian, Inc., Wallingford CT, **2009**.

[21] a) A. D. Becke, *J. Chem. Phys.* **1993**, *98*, 5648 – 5652; b) C. Lee, W. Yang, R. G. Parr, *Phys. Rev. B* **1988**, *37*, 785 – 789.

[22] S. Grimme, J. Antony, S. Ehrlich, H. Krieg, *J. Chem. Phys.* **2010**, *132*, 154104 – 154119.

[23] F. Weigend, R. Ahlrichs, *Phys. Chem. Chem. Phys.* **2005**, *7*, 3297 – 3305.

[24] J. W. McIver Jr, A. Komornicki, *J. Am. Chem. Soc.* **1972**, *94*, 2625 – 2633.

[25] C. Gonzalez, H. B. Schlegel, *J. Phys. Chem.* **1990**, *94*, 5523 – 5527.

Manuscript received: September 27, 2016
Accepted Article published: November 22, 2016
Final Article published: December 22, 2016